Van Med J 33 (1):45 -54, 2026
DOI: 10.5505/vmj.2026.43765

Cerebellar and Vermian Morphometry in Cadaveric Specimens: Reference Data for Posterior Fossa Approaches

Ufuk Erginoglu, Abdurrahman Aycan

University of Wisconsin School of Medicine, Department of Neurological Surgery, Public Health, Madison, WI, USA

Abstract

Introduction: The cerebellum, with the vermis central to posture and gait, is critical for posterior fossa and fourth ventricular surgery, where millimetric accuracy ensures safety. However, reference morphometric data remain inconsistent, particularly for vermian depth and proportional indices. This study aimed to establish reproducible cadaveric reference values through volumetric, linear, and proportional analyses.

Materials and Methods: Twenty-five formalin-fixed adult cerebellums were analyzed using volumetric displacement and standardized linear measurements. Proportional ratios were derived, and statistical comparisons were performed between hemispheres and across vermian levels.

Results: The right hemisphere was larger than the left in both volume (69.04 ± 4.56 vs 67.12 ± 4.39 mL) and width (49.00 ± 3.07 vs 47.08 ± 3.29 mm), with asymmetry indices of 1.41% and 2.02%. Volume correlation was strong ($r = 0.893$). Global shape ratios were stable, with height related to anteroposterior length ($r = 0.456$). Vermian dimensions were consistent (length 25.14 ± 2.49 mm; uvular width 14.88 ± 2.09 mm) and showed no significant rostrocaudal depth variation. Regression revealed scaling, with vermis length predicted by anteroposterior length ($\beta = 0.560$, $R^2 = 0.553$) and an inverse relation between anteroposterior length and uvular depth ($\beta = -0.169$, $R^2 = 0.248$).

Conclusion: These findings establish cadaveric reference values for the cerebellum and vermis, confirm mild right-sided asymmetry, and reveal stable proportions with coordinated scaling, including an inverse relationship between anteroposterior cerebellar elongation and uvular depth, thereby refining radiological interpretation and surgical planning.

Key words: Cadaver; cerebellum/anatomy & histology; cerebellar vermis/anatomy & histology; morphometrics/methods; reference values.

Introduction

The cerebellum plays a central role in motor coordination, balance, and higher cognitive processing, with the midline vermis being particularly important for posture and gait regulation (1, 2). Morphological variation in these regions has been linked to diverse clinical conditions, including ataxia, dementia, and congenital anomalies, such as the Dandy–Walker spectrum (3-8). Establishing reference morphometric data is therefore critical for distinguishing pathological alterations from normal anatomical variability. Precise cerebellar anatomy is equally critical for neurosurgical practice, particularly when addressing lesions of the posterior fossa and fourth ventricle. Several surgical corridors have been described. These include the transvermian approach (TVA), which involves splitting the vermis to gain direct access to the fourth ventricle, and the telovelar approach (TLA), which exploits the natural cleavage planes of the cerebellomedullary fissure to avoid midline splitting. Additional options include the supracerebellar–infratentorial approach (SCITA), most often applied for pineal and posterior mesencephalic lesions; the subtonsillar approach (STA), which provides access to the inferior fourth ventricle by mobilizing the tonsils; and the superior transvelar (STVA) and midline suboccipital keyhole approaches (MSKA), both designed to minimize tissue disruption while preserving neurological function(9-14). Detailed anatomical knowledge of cerebellar proportions and vermian depth is essential for safely navigating these approaches and minimizing operative morbidity. Although neuroimaging modalities such as magnetic resonance imaging (MRI) and computed tomography (CT) have facilitated noninvasive cerebellar morphometry, their precision often differs from that of direct cadaveric studies due to technical resolution and methodological variability (3, 5, 15-17). Previous cadaveric investigations have provided essential baseline data, but most have emphasized global

*Corresponding Author: Ufuk Erginoglu Neurosurgeon – Medical Scientist Mustafa K. Baskaya Lab, University of Wisconsin, School of Medicine & Public Health Department of Neurological Surgery 600 Highland Avenue, Clinical Science Center, K4/884 Madison, WI 53792, USA Email: erginoglu@wisc.edu **Orcid:** Ufuk Erginoglu 0000-0002-5387-4698 , Abdurrahman Aycan 0000-0002-3794-8511

Received: 27.08.2026, Accepted: 17.11.2026

dimensions or isolated landmarks without fully characterizing the proportional relationships between the hemispheres and vermis (4, 13, 18-20). This has left a gap in comprehensive reference datasets derived from anatomical series that integrate volumetric, linear, and proportional metrics across the entire cerebellum. The present study was designed to address this gap by systematically analyzing 25 formalin-fixed adult cadaveric specimens with intact cerebellum and brainstem. Through standardized measurements of global cerebellar dimensions, hemispheric volumes, and vermian parameters, we sought to establish morphometric reference values and proportional indices derived from an adult cadaveric series. These data provide not only an anatomical baseline for future clinical and radiological comparisons but also practical guidance for the selection and execution of surgical approaches to the posterior fossa and fourth ventricle.

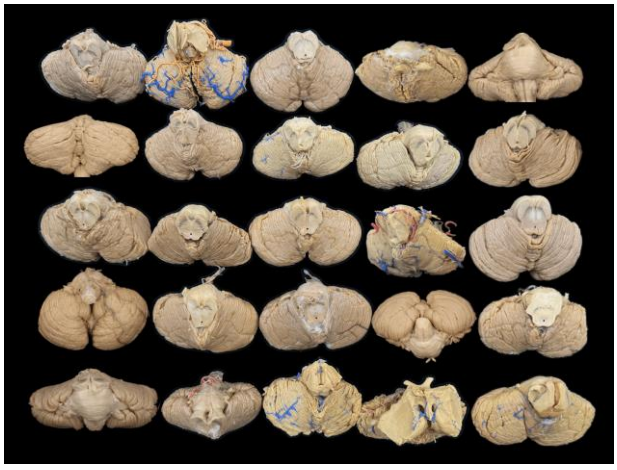

Figure 1: Gross anatomical view of the 25 formalin-fixed adult human brain specimens included in this study. Each specimen comprised an intact cerebellum, brainstem, and associated posterior fossa structures, with all cranial bones removed to permit direct visualization and morphometric analysis.

Materials and Methods

This anatomical study was conducted on 25 formaldehyde-fixed adult human brain specimens, each containing intact cerebellum, brainstem, and posterior fossa soft-tissue structures, with all cranial bones and cerebral hemispheres removed (Figure 1). The specimens were obtained in accordance with institutional policy. Under institutional guidelines, the use of cadaveric material for anatomical research purposes does not require separate ethics committee approval. Specimens with evidence of prior posterior fossa surgery, congenital anomalies, or distortion of cerebellar anatomy were excluded. All specimens were fixed in 10% formalin for a minimum of four weeks prior to analysis. Morphometric measurements focused on both global cerebellar dimensions and midline vermian anatomy. A total of twelve core variables were recorded. All linear measurements were obtained using digital Vernier calipers (accuracy ±0.01 mm), with the specimens positioned in a standardized anatomical orientation. Two observers independently verified each measurement to ensure consistency (Figures 2 and 3).

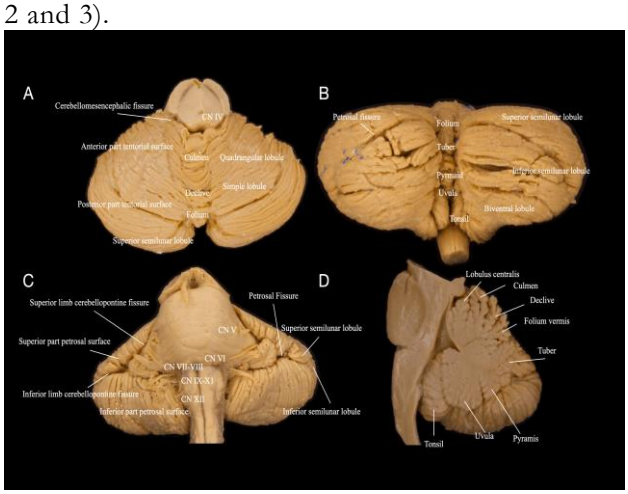

Figure 2: Figure 2. Serial dissections of the cerebellum and brainstem (A–D) demonstrate the principal anatomical landmarks used for orientation and measurement, including vermian lobules (culmen, declive, folium, tuber, uvula, pyramis), hemispheric lobules (quadrangular, semilunar, biventral, tonsil), and key fissures (cerebellomesencephalic, petrosal, cerebellopontine). These panels collectively illustrate the surfaces and reference points that guided morphometric analysis.

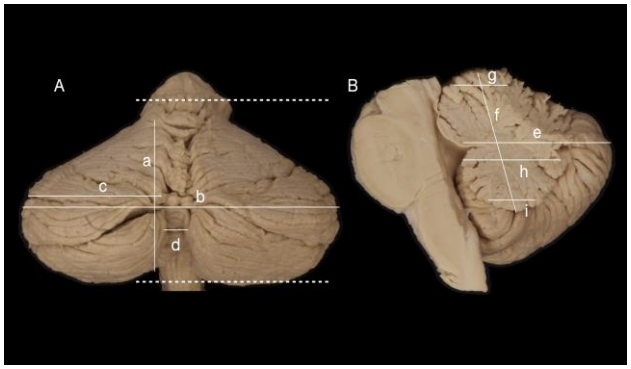

Figure 3: Morphometric landmarks used for cerebellar and vermian measurements. (A) a: whole-cerebellum height (apex of culmen to inferior tip of tonsils); b: whole-cerebellum width (maximal transverse span between lateralmost hemispheric margins with vermis re-approximated); c: right and left hemisphere widths (midline to lateralmost border of each hemisphere); d: vermis width at the uvula (maximal transverse span at that level). (B) e: whole-cerebellum anteroposterior length (anterior margin of culmen to posterior hemispheric contour); f: vermis length (culmen to nodulus); g: vermis depth at culmen; h: vermis depth at mid-vermis; i: vermis depth at uvula (all depths measured from dorsal cerebellar surface to ventricular floor)

Table 1: Descriptive Statistics of Cerebellar Morphometry in Adult Human Cadavers (n = 25)

Variable	Mean ± SD	Median	Range	IQR
Right cerebellar hemisphere volume (mL)	69.04 ± 4.56	68.0	18.0	6.0
Left cerebellar hemisphere volume (mL)	67.12 ± 4.39	68.0	16.0	6.0
Right cerebellar hemisphere width from midline (mm)	49.00 ± 3.07	49.0	13.0	4.0
Left cerebellar hemisphere width from midline (mm)	47.08 ± 3.29	47.0	15.0	3.0
Whole cerebellum width (mm)	101.44 ± 4.13	101.0	16.0	4.0
Whole cerebellum height (mm)	53.20 ± 3.85	54.0	13.0	6.0
Whole cerebellum anteroposterior length (mm)	52.52 ± 3.83	52.0	14.0	6.0
Vermis length (culmen → nodulus, mm)	44.36 ± 2.89	44.0	10.0	4.0
Vermis width at uvula (mm)	13.96 ± 1.54	14.0	5.0	2.0
Vermis depth at culmen (mm)	26.12 ± 2.51	26.0	10.0	3.0
Vermis depth at mid-vermis (mm)	24.40 ± 1.68	24.0	6.0	3.0
Vermis depth at uvula (mm)	23.12 ± 1.30	23.0	5.0	2.0

Abbreviations: SD = standard deviation; IQR = interquartile range. Descriptive statistics were calculated for all variables using both parametric (mean ± SD) and non-parametric (median, IQR, range) methods. Normality was assessed using the Shapiro–Wilk test. Measurement landmarks and axis definitions are provided in the Morphometric Methods section.

Global cerebellar dimensions included the whole cerebellum width, defined as the maximal transverse extent between the lateralmost hemispheric margins with the vermis re-approximated; the whole cerebellum height, measured from the apex of the culmen to the inferior tip of the tonsils in the midline; and the whole cerebellum anteroposterior length, measured in the midsagittal plane from the anterior point of the culmen to the most posterior contour of the cerebellar surface. Right and left cerebellar hemisphere widths were measured from the midline to the lateralmost extent of each hemisphere. Volumes of the right and left cerebellar hemispheres were calculated using the water displacement method in a graduated cylinder (Figure 3). Vermis-specific parameters included the length of the vermis from the culmen to the nodulus, measured as the straight-line (Euclidean) distance between these two landmarks using digital calipers. Vermis width at the uvula was defined as the maximal transverse span of the vermis at that level. Vermis depth was assessed at three midline levels—culmen, mid-vermis, and uvula—by measuring the distance from the dorsal surface to the ventricular floor (Figure 3).

Ethical Approval: All cadaveric specimens were obtained through the University of Wisconsin–Madison anatomical donation program, were fully anonymized, and contained no identifiable personal or clinical information. Specimen handling complied with institutional and ethical standards. In accordance with University of Wisconsin–Madison policy, anatomical studies using donated, anonymized cadaveric material are exempt from institutional review board approval.

Statistical Analysis: All statistical analyses were conducted using Python (v3.10) and the following packages: pandas, scipy, and statsmodels. Descriptive statistics were computed for all variables using both parametric (mean ± standard deviation [SD]) and non-parametric (median, interquartile range [IQR], and range) methods. The Shapiro–Wilk test was used to assess normality. Paired t-tests (PTT) were used to compare right and left cerebellar hemisphere volumes and widths after confirming normality. The asymmetry index (AI) was calculated using the formula: (Right − Left) / (Right + Left) × 100. Pearson correlation coefficients (PCCs) were calculated to assess linear associations among global cerebellar dimensions, as well as inter-hemispheric correlations between right and left hemisphere volumes and widths. Global cerebellar shape ratios, including width/height, width/length, and height/length, were computed and reported along with SD and coefficient of variation (CV). Vermian dimensions were scaled to their corresponding cerebellar dimensions to generate proportional ratios. These were analyzed using descriptive statistics, and paired t-tests were used to compare vermis depths at the culmen, mid-vermis, and uvula levels. P-values were adjusted using the Bonferroni correction (BC) for multiple comparisons. To assess predictive relationships, linear regression models were constructed with vermian morphometric variables as dependent outcomes and global cerebellar dimensions as predictors. Each model was labeled according to whether the predictor corresponded to a matched anatomical axis (e.g., vertical, transverse, or anteroposterior) relative to the vermis variable. Statistical significance was defined as $p < 0.05$.

Results

Descriptive morphometry: The mean right cerebellar hemisphere volume was 69.04 ± 4.56 mL, while the left measured 67.12 ± 4.39 mL. Hemisphere widths from the midline averaged 49.00 ± 3.07 mm on the right and 47.08 ± 3.29 mm on the left. The mean whole cerebellum width was 101.44 ± 4.13 mm; height, 53.20 ± 3.85 mm; and anteroposterior (AP) length, 52.52 ± 3.83 mm (Table 1).

Table 2: Cerebellar Hemisphere Symmetry and Global Shape Ratios

Section A – Right vs. Left Hemisphere Comparisons (paired t-test)				
Variable	**Right Side Mean ± SD**	**Left Side Mean ± SD**	**Asymmetry Index (% Mean ± SD)**	**p-value (paired t-test)**
Cerebellar hemisphere volume (mL)	69.04 ± 4.56	67.12 ± 4.39	1.41 ± 1.52	< 0.001
Cerebellar hemisphere width from midline (mm)	49.00 ± 3.07	47.08 ± 3.29	2.02 ± 3.50	0.011

Section B – Inter-Hemispheric Correlation

Comparison	**Pearson r**	**p-value**
Volume (Right vs. Left)	0.893	< 0.001
Width (Right vs. Left)	0.409	0.043

Section C – Global Cerebellar Shape Ratios

Ratio	**Mean**	**SD**	**CV (%)**
Cerebellar hemisphere Width / Height	1.917	0.160	8.3%
Cerebellar hemisphere Width / Length	1.942	0.166	8.6%
Cerebellar hemisphere Height / Length	1.016	0.082	8.1%

Section D – Correlation Among Global Cerebellar Dimensions

Dimension Pair	**Pearson r**	**p-value**
Cerebellar hemisphere Width vs. Height	-0.019	0.9288
Cerebellar hemisphere Width vs. Length	-0.068	0.7479
Cerebellar hemisphere Height vs. Length	0.456	0.0220

Abbreviations: SD = standard deviation; CV = coefficient of variation. Paired t-tests were used to compare right and left cerebellar hemisphere volume and width after confirming normality, with asymmetry indices calculated as ((Right – Left) / (Right + Left)) × 100. Pearson correlation coefficients were used to assess inter-hemispheric associations between right and left hemisphere volume and width, as well as relationships among global cerebellar dimensions. Global cerebellar shape ratios (width/height, width/length, height/length) are reported as mean, SD, and CV. Significant p-values ($p < 0.05$) are shown in bold.

Global cerebellar morphometry and Inter-hemispheric comparisons: Across 25 adult specimens, the mean volume of the right cerebellar hemisphere was significantly larger than the left (69.04 ± 4.56 mL vs. 67.12 ± 4.39 mL; $p < 0.001$). Similarly, the mean width from the midline to the lateralmost margin was greater on the right side (49.00 ± 3.07 mm vs. 47.08 ± 3.29 mm; $p = 0.011$). These differences yielded AIs of 1.41 ± 1.52% for volume and 2.02 ± 3.50% for width, confirming a mild but statistically significant right-sided lateralization (Table 2, Section A). Strong inter-hemispheric correlation was observed for hemisphere volume (PCC = 0.893, $p < 0.001$), and moderate correlation was found for width (PCC = 0.409, $p = 0.043$), indicating that larger structures on one side tend to be mirrored by the contralateral side (Table 2, Section B). These relationships support intrinsic bilateral symmetry in cerebellar development, with modest lateral variation.

Cerebellar shape ratios and proportional relationships: Cerebellar shape was further characterized using three proportional indices. The mean width-to-height ratio was 1.917 ± 0.160, width-to-length was 1.942 ± 0.166, and

height-to-length was 1.016 ± 0.082. The low CVs (8.1%–8.6%) for these ratios indicate that global cerebellar shape remains relatively stable across individuals. PCC analysis revealed no significant association between width and height ($r = -0.019$, $p = 0.9288$) or width and length ($r = -0.068$, $p = 0.7479$), suggesting transverse expansion does not necessarily track with other dimensions. However, a moderate positive correlation was observed between height and length ($r = 0.456$, $p = 0.0220$), suggesting that vertical and anteroposterior dimensions tend to scale together (Table 2, Sections C and D).

Table 3: Vermis Proportional Scaling and Depth Comparisons

Section A – Proportional Vermis Dimensions			
Proportion	**Mean (%)**	**SD (%)**	**CV (%)**
Vermis length (culmen → nodulus, mm) / Whole cerebellum height (mm)	84.61	4.24	5.0
Vermis width at uvula (mm) / Whole cerebellum width (mm)	13.80	1.81	13.1
Vermis depth at culmen (mm) / Whole cerebellum anteroposterior length (mm)	49.33	5.77	11.7
Vermis depth at mid-vermis (mm) / Whole cerebellum anteroposterior length (mm)	46.17	5.36	11.6
Vermis depth at uvula (mm) / Whole cerebellum anteroposterior length (mm)	43.77	4.89	11.2
Section B – Internal Vermis Depth Comparison			
Comparison	t-statistic	p-value (Bonferroni)	
Culmen vs Mid-vermis	3.114	0.014	
Culmen vs Uvula	4.910	< 0.001	
Mid-vermis vs Uvula	3.483	0.006	

Abbreviations: SD = standard deviation; CV = coefficient of variation. Section A reports vermian dimensions scaled to their anatomically corresponding whole cerebellar axes, with proportional ratios presented as mean, SD, and CV. Section B compares vermis depths at the culmen, mid-vermis, and uvula levels using paired t-tests; p-values were Bonferroni-adjusted. Significant results ($p < 0.05$) are shown in bold.

Vermian morphometry and proportional scaling: Absolute vermian dimensions were consistent across specimens. The mean vermis length (culmen to nodulus) was 25.14 ± 2.49 mm, and the vermis width at the uvula measured 14.88 ± 2.09 mm. Vermis depth varied modestly across the midline: it was deepest at the mid-vermis (10.97 ± 1.75 mm), followed by the culmen (10.33 ± 1.90 mm), and shallowest at the uvula (8.92 ± 1.84 mm) (Table 1). To account for variability in global cerebellar size, vermian dimensions were normalized to the corresponding cerebellar axes. These proportional ratios exhibited low CVs (9.0%-13.7%), indicating consistent scaling across specimens. When compared using PTT, no statistically significant differences were observed among vermis depths at the culmen, mid-vermis, and uvula following BC, supporting a relatively symmetric depth distribution along the midline vermis (Table 3, Sections A and B).

Regression analysis of vermis–cerebellum relationships: Linear regression models were used to test whether global cerebellar dimensions could predict vermian morphometry. When anatomical axes were matched (e.g., height predicting depth), only one significant finding emerged: greater cerebellar anteroposterior length predicted reduced vermis depth at the uvula ($\beta = -0.169$, $R^2 = 0.248$, $p = 0.011$), possibly reflecting morphological compression or elongation effects along the posterior fossa's sagittal plane (Table 4, Figure 4). In contrast, several statistically significant associations were identified when axes were crossed. Vermis length was strongly predicted by cerebellar anteroposterior length ($\beta = 0.560$, $R^2 = 0.553$, $p < 0.001$), indicating a coordinated growth pattern along the midline. Vermis width at the uvula also showed positive correlations with cerebellar anteroposterior length ($\beta = 0.266$, $R^2 = 0.436$, $p < 0.001$) and cerebellar height ($\beta = 0.172$, $R^2 = 0.185$, $p = 0.032$). These cross-axis relationships suggest that certain vermian parameters, particularly width and length, may be influenced by broader cerebellar growth

Table 4: Linear Regression of Vermis Morphometry on Global Cerebellar Dimensions

Dependent Variable	Predictor (Global Cerebellar Axis)	β Coefficient	R^2	p-value	Matched Anatomical Axis
Vermis length (culmen → nodulus, mm)	Whole cerebellum height (mm)	0.090	0.015	0.565	Yes
Vermis width at uvula (mm)	Whole cerebellum width (mm)	0.039	0.007	0.694	Yes
Vermis depth at culmen (mm)	Whole cerebellum anteroposterior length (mm)	0.075	0.013	0.585	Yes
Vermis depth at mid-vermis (mm)	Whole cerebellum anteroposterior length (mm)	-0.086	0.038	0.350	Yes
Vermis depth at uvula (mm)	Whole cerebellum anteroposterior length (mm)	-0.169	0.248	0.011	Yes
Vermis length (culmen → nodulus, mm)	Whole cerebellum anteroposterior length (mm)	0.560	0.553	< 0.001	No
Vermis width at uvula (mm)	Whole cerebellum height (mm)	0.172	0.185	0.032	No
Vermis width at uvula (mm)	Whole cerebellum anteroposterior length (mm)	0.266	0.436	< 0.001	No
Vermis depth at uvula (mm)	Whole cerebellum height (mm)	-0.167	0.246	0.012	No

Linear regression models assess the relationship between vermian morphometry and global cerebellar dimensions. 'Matched Anatomical Axis' indicates whether the predictor corresponds to the expected spatial orientation of the vermis variable (e.g., vertical, transverse, or anteroposterior). Significant p-values ($p < 0.05$) are in bold.

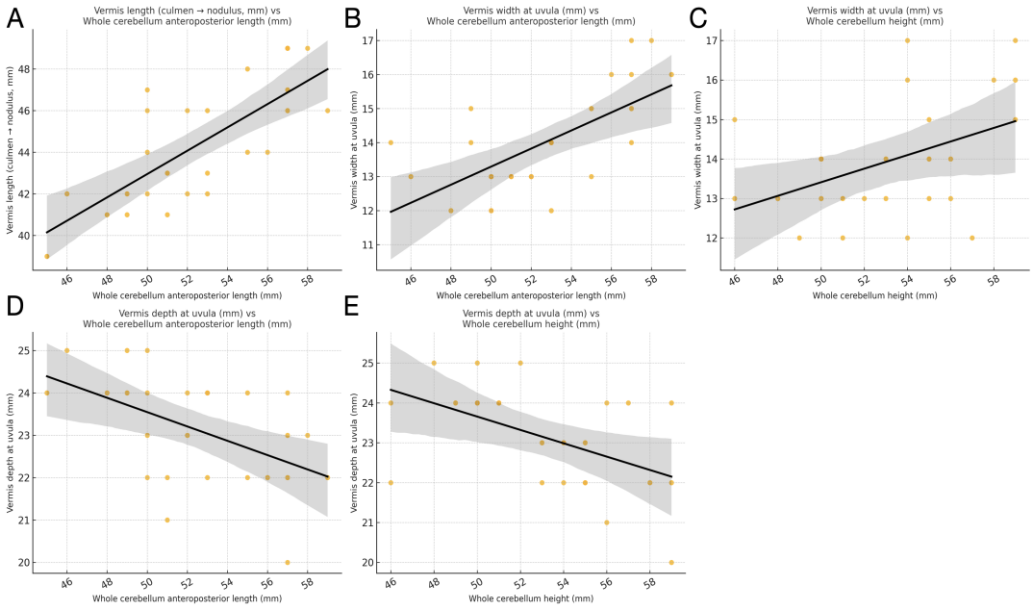

Figure 4: Linear regression analysis of vermian–cerebellar relationships. Scatter plots with fitted regression lines (black) and 95% confidence intervals (gray shading) demonstrate proportional associations between vermian and global cerebellar dimensions across 25 specimens. (A) Vermis length (culmen → nodulus) versus whole cerebellum anteroposterior length; (B) vermis width at the level of the uvula versus anteroposterior length; (C) vermis width at the uvula versus whole cerebellum height. (D) Vermis depth at the uvula versus anteroposterior length; (E) vermis depth at the uvula versus whole cerebellum height. Positive correlations were observed for vermis length and width, whereas vermis depth at the uvula demonstrated an inverse relationship with cerebellar size.

dynamics, rather than strictly adhering to their corresponding spatial axis (Table 4, Figure 4).

Discussion

The cerebellum is an anatomically compact yet functionally diverse structure, with the vermis at its center playing a pivotal role in posture, balance, and coordination (10, 21). For neurosurgeons, precise knowledge of its morphology is indispensable when planning posterior fossa approaches, particularly to the fourth ventricle, where millimeters can determine the margin between safe dissection and neurological deficit. In tumors, vascular lesions, or congenital anomalies, local anatomy may be distorted, and the surgeon must rely on dependable reference values derived from anatomical series to distinguish between actual pathology and normal variation. This makes accurate morphometric data not simply descriptive but directly operative in value. In daily practice, surgeons rely on both radiological interpretation and intraoperative anatomy, yet reference morphometric datasets remain limited and often inconsistent across modalities. MRI and CT studies have provided large-scale volumetric benchmarks, but they frequently lack the resolution to delineate vermian depth and proportional indices with accuracy, while earlier cadaveric series emphasized isolated dimensions without integrating volumetric or proportional analysis (3-5, 13, 22-24). Recent cadaveric volumetric work, including our study of cerebellar tonsillar morphology, has similarly focused on regional anatomy rather than whole-cerebellum or vermian proportional relationships (25). By bridging this gap, our cadaveric dataset provides anatomical constants that anchor intraoperative orientation and enhance the accuracy of MRI-based neuronavigation, a process in which millimetric precision is crucial for surgical safety.

Our cadaveric dataset addresses these limitations by combining volumetric displacement, linear morphometry, and proportional ratios to generate reproducible anatomical constants. By systematically quantifying cerebellar hemisphere volumes, global cerebellar ratios, and vermian dimensions, we provide a framework that strengthens the baseline against which both imaging studies and intraoperative findings can be interpreted. Beyond its descriptive value, this dataset carries direct surgical implications: understanding expected anatomical variation allows neurosurgeons to distinguish true pathological distortion from normal asymmetry, and it informs the planning of critical midline and fourth ventricular approaches such as the TVA, TLA, STA, STVA, MSKA, and SCITA (9, 10, 12, 13).

Cerebellar hemisphere asymmetry and bilateral correlation: In our series, the right cerebellar hemisphere was significantly larger than the left in both volume (69.04 ± 4.56 mL vs. 67.12 ± 4.39 mL, $p < 0.001$) and width (49.00 ± 3.07 mm vs. 47.08 ± 3.29 mm, $p = 0.011$). The corresponding asymmetry indices were 1.41% for volume and 2.02% for width, with strong interhemispheric correlation for volume (PCC = 0.893, $p < 0.001$) and moderate correlation for width (PCC = 0.409, $p = 0.043$). These findings are in line with MRI studies that consistently report mild rightward asymmetry within the range of one to three percent and robust bilateral coupling (3, 5, 8, 23, 24, 26). Earlier cadaveric reports observed similar trends but with wider variability, likely due to reliance on caliper-based methods and small sample sizes (4, 13, 19). For clinical practice, the importance lies not in the presence of asymmetry itself—which is a normal feature—but in recognizing its narrow limits. Volumes or widths deviating substantially beyond this baseline should alert the surgeon or radiologist to unilateral atrophy, mass effect, or postsurgical change. In operative settings, such as tumor resection or Chiari decompression, understanding this physiologic asymmetry prevents overinterpretation of minor lateral differences as pathological.

Global cerebellar shape and proportional ratios: The global geometry of the cerebellum was conserved across specimens. The mean width-to-height ratio was 1.917 ± 0.160, width-to-length was 1.942 ± 0.166, and height-to-length was 1.016 ± 0.082, all with coefficients of variation between 8.1% and 8.6%. Height and anteroposterior length were positively correlated ($r = 0.456$, $p = 0.022$), while width showed no significant relationship to either parameter. These findings suggest that vertical and sagittal growth are developmentally coupled, whereas the transverse axis evolves more independently. Comparable proportional stability has been described in anatomical and imaging surveys, supporting the idea that adult cerebellar geometry is highly conserved (13, 18, 19, 27, 28). For the neurosurgeon, this stability is particularly valuable during restricted approaches such as the MSKA or SCITA, where only part of the cerebellar surface may be visible. Proportional ratios, rather than absolute values, allow intraoperative estimation of hidden dimensions and facilitate safe dissection trajectories even in

patients with overall smaller or larger posterior fossae.

Vermian morphometry and surgical landmarks: The vermis showed consistent dimensions across specimens, with a mean length of 25.14 ± 2.49 mm and a width at the uvula of 14.88 ± 2.09 mm. Depth was 10.33 ± 1.90 mm at the culmen, 10.97 ± 1.75 mm at the mid-vermis, and 8.92 ± 1.84 mm at the uvula. After Bonferroni correction, these rostrocaudal differences were not statistically significant, supporting a balanced depth profile. However, this lack of statistical significance should be interpreted cautiously, as the conservative nature of the Bonferroni adjustment in a modest sample (n = 25) may have reduced statistical power and obscured subtle differences in anatomical depth. These values align with postmortem and histological reports, while adding systematic depth of data that earlier works often lacked (4, 12, 13, 19, 29). This information has direct surgical relevance. In TVA and STVA corridors, operative entry often traverses specific vermian segments, and accurate knowledge of depth is crucial to avoid injury to fastigial or dentate nuclei. While earlier literature described the vermis qualitatively, our reproducible depth profiles provide quantitative guidance for incision planning. The translation of these findings is further supported by MRI studies that report compatible midsagittal vermis dimensions (2, 24, 30, 31), reinforcing their utility in preoperative imaging review and neuronavigation.

Predictive relationships between vermis and cerebellum: Our regression analyses demonstrated clear scaling relationships. Vermis length correlated strongly with anteroposterior cerebellar length ($\beta = 0.560$, $R^2 = 0.553$, $p < 0.001$), while vermis width correlated with both anteroposterior length and height ($\beta = 0.266$ and 0.172, $R^2 = 0.436$ and 0.185, $p < 0.001$ and $p = 0.032$). Notably, greater anteroposterior length predicted reduced uvular depth ($\beta = -0.169$, $R^2 = 0.248$, $p = 0.011$), suggesting an inverse relationship between elongation and inferior vermian concavity. This inverse relationship may reflect broader geometric and developmental constraints of the posterior fossa. Prior radiological studies have shown that individuals with a more elongated posterior fossa axis tend to exhibit reduced inferior vermian concavity, suggesting that global sagittal expansion can produce a relative flattening of the uvula (3, 23, 26). Embryological and developmental analyses have also demonstrated that hemispheric growth progresses more rapidly and laterally than inferior vermian maturation, which may contribute to a shallower uvula in specimens with proportionally longer anteroposterior dimensions (21, 22). Although these mechanisms remain theoretical, they provide a plausible anatomical context for our findings and justify further investigation using large-scale MRI-based morphometric datasets.

This contrasts with older cadaveric series, which considered vermian and hemispheric growth largely independent (13, 18, 30). The newly identified inverse relation between anteroposterior elongation and uvular depth warrants confirmation in larger radiological datasets; however, if validated, it may represent an anatomical principle with clinical impact (3, 5, 26). For instance, in planning TVA or STVA exposures, surgeons encountering a longer posterior fossa axis should anticipate a shallower uvula, which guides dissection depth and reduces the risk of injury to midline nuclei.

Integration with clinical and radiological literature: Taken together, our findings reinforce and extend the existing literature. Imaging studies confirm mild rightward asymmetry and proportional stability but are limited in their ability to assess vermian depth or proportional indices with precision (3, 26). Our cadaveric dataset, by incorporating volumetric displacement and direct linear measurements, provides the anatomical resolution necessary to refine these baselines. From a clinical perspective, these constants establish a reference for evaluating conditions that disproportionately involve the vermis and midline structures. Alcohol-related degeneration, congenital anomalies such as Dandy–Walker malformation, and neurodegenerative syndromes with cerebellar involvement all manifest with vermian distortion that exceeds normal variation (1, 2, 4, 6, 7). Establishing the narrow reference ranges derived from this anatomical series ensures that physiologic asymmetry or proportional variation is not misinterpreted as pathological, while actual deviations can be recognized with greater confidence.

Study Limitations: This study is limited by a modest sample size, the absence of demographic stratification, and the potential for formalin fixation to induce tissue shrinkage. In addition, because demographic variables such as age and sex were not available for the specimens, the measurements cannot be interpreted as normative population-wide values; instead, they should be considered reference morphometric data derived from a cadaveric anatomical series. However, standardized fixation, proportional indices, and

displacement volumetry provide precision beyond caliper-only methods, ensuring the robustness and clinical applicability of the reported reference values. Future imaging-based studies can extend these cadaveric constants into larger and demographically stratified populations, reinforcing their utility across diverse clinical settings.

Conclusion

This cadaveric study establishes reference morphometric measurements for the cerebellum and vermis, integrating volumetric, linear, proportional, and regression-based indices. The data confirm small but significant rightward asymmetry, stable global shape ratios with low coefficients of variation, and predictable scaling between vermian parameters and global cerebellar size, including a newly observed inverse relationship between anteroposterior length and uvular depth. These constants refine radiological interpretation and provide practical anatomical guidance for neurosurgeons performing posterior fossa and fourth ventricular approaches.

Acknowledgments: The authors thank Professor Mustafa K. Baskaya for his expert mentorship and guidance throughout the development of this study. The authors also acknowledge the generous contribution of the individuals who donated their bodies for anatomical research and express gratitude to their families.

Ethical approval: The study was conducted on de-identified cadaveric specimens in accordance with institutional policy and was exempt from formal ethics committee approval. No living human participants or animals were involved.

Conflict of interest: The authors declare no conflict of interest.

Financial support: This research received no specific grant from any funding agency.

Author Contributions: Conceptualization/Design: U.E. Data Collection: U.E. Analysis/Interpretation: U.E., A.A. Drafting of Manuscript: U.E. Critical Revision: All authors Final Approval: All authors terior fossa and fourth ventricular approaches.

References

1. Ding H, Qin W, Jiang T, Zhang Y, Yu C. Volumetric variation in subregions of the cerebellum correlates with working memory performance. Neurosci Lett. 2012;508(1):47-51.
2. Oksuzler M, Oksuzler Y, Tune M, Polat S, Vuralli D, Goker P. The Evaluation of Cer ebellum Gross Morphometric Measur ements in Subjects Having Migraine, Ataxia, Dementia, and Vertigo. Int. J. Morphol. 2022;40(4).
3. Luft AR, Skalej M, Welte D, Kolb R, Bürk K, Schulz JB, et al. A new semiautomated, three-dimensional technique allowing precise quantification of total and regional cerebellar volume using MRI. Magn Reson Med. 1998;40(1):143-51.
4. Direković R, Bečulić H, Krivokuća Z. Correlation of the inclination of the tentorium cerebellum and the volume of the posterior cranial fossa. Med Glas (Zenica). 2023;20(2):112-6.
5. Keller A, Castellanos FX, Vaituzis AC, Jeffries NO, Giedd JN, Rapoport JL. Progressive loss of cerebellar volume in childhood-onset schizophrenia. Am J Psychiatry. 2003;160(1):128-33.
6. Acar M, Seker B, Ugur S. Radio-Anatomical Assessment of Cerebellum Volume in Individuals with Alzheimer's Disease. Curr Alzheimer Res. 2024;21(8):599-606.
7. Melgaard B, Ahlgren P. Ataxia and cerebellar atrophy in chronic alcoholics. J Neurol. 1986;233(1):13-5.
8. Murakami JW, Courchesne E, Press GA, Yeung-Courchesne R, Hesselink JR. Reduced cerebellar hemisphere size and its relationship to vermal hypoplasia in autism. Arch Neurol. 1989;46(6):689-94.
9. Tanriover N, Ulm AJ, Rhoton AL, Jr., Yasuda A. Comparison of the transvermian and telovelar approaches to the fourth ventricle. J Neurosurg. 2004;101(3):484-98.
10. Rhoton AL, Jr. Cerebellum and fourth ventricle. Neurosurgery. 2000;47(3 Suppl):S7-27.
11. Mussi AC, Rhoton AL, Jr. Telovelar approach to the fourth ventricle: microsurgical anatomy. J Neurosurg. 2000;92(5):812-23.
12. Spierer R. The debated neuroanatomy of the fourth ventricle. J Anat. 2023;243(4):555-63.
13. Lang J, Jr., Ohmachi N, Lang J, Sr. Anatomical landmarks of the Rhomboid fossa (floor of the 4th ventricle), its length and its width. Acta Neurochir (Wien). 1991;113(1-2):84-90.
14. Dang DD, Rechberger JS, Leonel L, Hallak H, Graepel S, Link MJ, et al. Anatomical Step-by-Step Dissection of Midline Suboccipital Approaches to the Fourth Ventricle for Trainees: Surgical Anatomy of the Telovelar, Transvermian, and Superior

Transvelar Routes, Surgical Principles, and Illustrative Cases. J Neurol Surg B Skull Base. 2024;85(2):172-88.
15. Woodruff-Pak DS, Vogel RW, 3rd, Ewers M, Coffey J, Boyko OB, Lemieux SK. MRI-assessed volume of cerebellum correlates with associative learning. Neurobiol Learn Mem. 2001;76(3):342-57.
16. Rhyu IJ, Cho TH, Lee NJ, Uhm CS, Kim H, Suh YS. Magnetic resonance image-based cerebellar volumetry in healthy Korean adults. Neurosci Lett. 1999;270(3):149-52.
17. Perera IR, Zahed M, Moriarty S, Simmons Z, Rodriguez M, Botkin C, et al. Geometric morphometric analysis of the brainstem and cerebellum in Chiari I malformation. Front Neuroanat. 2024; 18:1434017.
18. Last RJ, Tompsett DH. Casts of the cerebral ventricles. Br J Surg. 1953;40(164):525-43.
19. Umarani S, Arjun R, Kumar S, Sivaraj R. Morphometric assessment of the external anatomy of fourth ventricle & dorsal brainstem in South Indian population. Int J Health Sci. 2022;6(S6):9609-14.
20. Lv M, Yang X, Zhou X, Chen J, Wei H, Du D, et al. Gray matter volume of cerebellum associated with idiopathic normal pressure hydrocephalus: A cross-sectional analysis. Front Neurol. 2022; 13:922199.
21. Dow RS. The evolution and anatomy of the cerebellum. Biological reviews. 1942;17(3):179-220.
22. Huttenlocher PR. Morphometric study of human cerebral cortex development. Neuropsychologia. 1990;28(6):517-27.
23. Jandeaux C, Kuchcinski G, Ternynck C, Riquet A, Leclerc X, Pruvo J-P, et al. Biometry of the cerebellar vermis and brain stem in children: MR imaging reference data from measurements in 718 children. AJNR Am J of Neuroradiol. 2019;40(11):1835-41.
24. Murshed KA, Ziylan T, Seker M, Cicekcibasi AE, Acikgozoglu S. Morphometric assessment of brain stem and cerebellar vermis with midsagittal MRI: the gender differences and effects of age. Neuroanatomy. 2003; 2:35-8.
25. Erginoglu U, Aycan A. Normative Cerebellar Tonsil Morphology: A Cadaveric Study of Bilateral Volume, Shape, and Three-Dimensional Spatial Relationships. Eastern J Med. 2025;30(4):602-9.
26. Raz N, Dupuis JH, Briggs SD, McGavran C, Acker JD. Differential effects of age and sex on the cerebellar hemispheres and the vermis: a prospective MR study. AJNR Am J Neuroradiol. 1998;19(1):65-71.
27. Antar V, Turk O, Katar S, Ozden M, Sahin B, Yuceli S, et al. Morphometric Assesment of the External Anatomy of Fourth Ventricle and Dorsal Brainstem in Fresh Cadavers. Turk Neurosurg. 2019;29(3):445-50.
28. Edwards CR, Newman S, Bismark A, Skosnik PD, O'Donnell BF, Shekhar A, et al. Cerebellum volume and eyeblink conditioning in schizophrenia. Psychiatry Res. 2008;162(3):185-94.
29. Ahmad N, Singh D, Jethani SL. Role of Vermal Anteroposterior Length and Width in Age Determination of Fetus. J Anat Soc India. 2023;72(2):135-9.
30. Metwally MI, Basha MAA, AbdelHamid GA, Nada MG, Ali RR, Frere RAF, et al. Neuroanatomical MRI study: reference values for the measurements of brainstem, cerebellar vermis, and peduncles. Br J Radiol. 2021;94(1120):20201353.
31. Cignini P, Giorlandino M, Brutti P, Mangiafico L, Aloisi A, Giorlandino C. Reference charts for fetal cerebellar vermis height: a prospective cross-sectional study of 10605 fetuses. Plos One. 2016;11(1):e0147528.